

ENHANCING THE OPERATIONAL STABILITY OF RECOMBINANT PHENYLALANINE AMMONIA-LYASE IMMOBILIZED ON MAGNETIC NANOPARTICLES BY POST-ENTRAPMENT

Bálint ALÁCS^a, Anna ZRINYI^a, Evelin BELL^{a,*} 

ABSTRACT. Recombinant *Petroselinum crispum* phenylalanine ammonia-lyase (PcPAL) was selectively immobilized on magnetic nanoparticles by metal affinity binding (IMAC) to create a well applicable biocatalyst. To overcome the stability limitations of coordination bond, two post-immobilization entrapment strategies were investigated: macroscopic entrapment in calcium-alginate hydrogel beads and also in sol–gel matrix. The catalytic efficiency and operational stability of the composite biocatalysts were evaluated in the ammonia elimination reaction of L-phenylalanine. The concentration of immobilized biocatalyst was optimized in the calcium-alginate stabilization. In the sol–gel shell formation the amount of tetraethyl ortosilicate (TEOS) and the combination with a less crosslinking capability dimethyldiethoxysilane (DMDEOS) was investigated. In the latter case the TEOS was used in 4 different ratios in the silane precursor mixture. While the best calcium-alginate beads (5 m/m% loading) provided a biocompatible environment, they suffered from mechanical instability and physical disintegration occur after four reaction cycles. In contrast, the optimized silica-coated nanobiocatalyst exhibited superior mechanical and chemical stability, preventing enzyme leaching and retaining over 80% of its initial activity after seven consecutive reaction cycles. These results demonstrate that individual particle encapsulation via a silica shell offers a more robust solution for the design of reusable magnetic biocatalysts than macroscopic hydrogel entrapment.

Keywords: *immobilized metal ion affinity chromatography, enzyme immobilization, sol-gel, alginate*

^a Department of Organic Chemistry and Technology, Faculty of Chemical Technology and Biotechnology, Budapest University of Technology and Economics, Műegyetem rkp. 3., H-1111 Budapest, Hungary

* Corresponding author: bell.evelin@vbk.bme.hu



INTRODUCTION

Biocatalysis has been getting a growing focus in sustainable industrial chemistry, offering highly stereo- and regioselective routes to valuable compounds under mild reaction conditions [1–3]. Enzymes, such as phenylalanine ammonia-lyase (PAL), are widely used in the synthesis of pharmaceutical intermediates and amino acids [4]. However, the industrial application of soluble enzymes is often hampered by their high production costs, low stability under process conditions, and the difficulty of their recovery [5]. Enzyme immobilization provides a robust solution to these challenges, enabling facile separation, catalyst recycling, and often improved thermal and operational stability [6].

Among the various support materials, magnetic nanoparticles (MNPs) have gained significant attention due to their high specific surface area and the ease of separation using an external magnetic field, which eliminates the need for filtration or centrifugation [7,8]. Due to their advantageous applicability, they are also used in combined enzyme immobilization processes, such as in the formation of magnetic nanoparticle supported cross-linked enzyme aggregates [9]. For the immobilization of recombinant enzymes, Immobilized Metal Affinity Chromatography (IMAC) offers a unique advantage: It allows for the selective binding of histidine-tagged (His-tagged) proteins directly from crude cell lysates [10]. This “one-pot” purification and immobilization strategy significantly reduces the time and cost of biocatalyst preparation compared to traditional methods that require prior enzyme purification [11].

Despite its efficiency, traditional IMAC-based immobilization has limitations. The metal-coordination bond can be susceptible to ligand exchange or metal ion leaching during operation, leading to enzyme detachment and product contamination [12]. Furthermore, enzymes bound solely to the surface of nanoparticles remain exposed to shear forces and harsh solvent environments. To address these issues, post-immobilization stabilization strategies are required to shield the biocatalyst while maintaining the benefits of the magnetic support [13].

In this study, we present the development of robust magnetic nanoparticles-based biocatalysts using recombinant *Petroselinum crispum* phenylalanine ammonia-lyase [14] (*PcPAL*) selectively immobilized via metal affinity binding. To overcome the stability limitations of simple surface binding, we investigated and compared two distinct entrapment strategies. The first approach involved the macroscopic entrapment of the enzyme-loaded nanoparticles into calcium-alginate beads to create a biocompatible diffusion barrier. In parallel, we examined microscopic encapsulation by forming a porous silica shell directly around the enzyme-coated nanoparticles, resulting in individual

ENHANCING THE OPERATIONAL STABILITY OF RECOMBINANT PHENYLALANINE AMMONIA-LYASE IMMOBILIZED ON MAGNETIC NANOPARTICLES BY POST-ENTRAPMENT

core-shell nanostructures (Figure 1.). We examined the morphological properties of the resulting composites and evaluated their catalytic efficiency, kinetic parameters, and reusability in the ammonia elimination reaction of L-phenylalanine, resulting (*E*)-cinnamic acid [15]. Our results provide insights into the trade-offs between mass transfer limitations and structural stability in the design of magnetically separable biocatalysts.

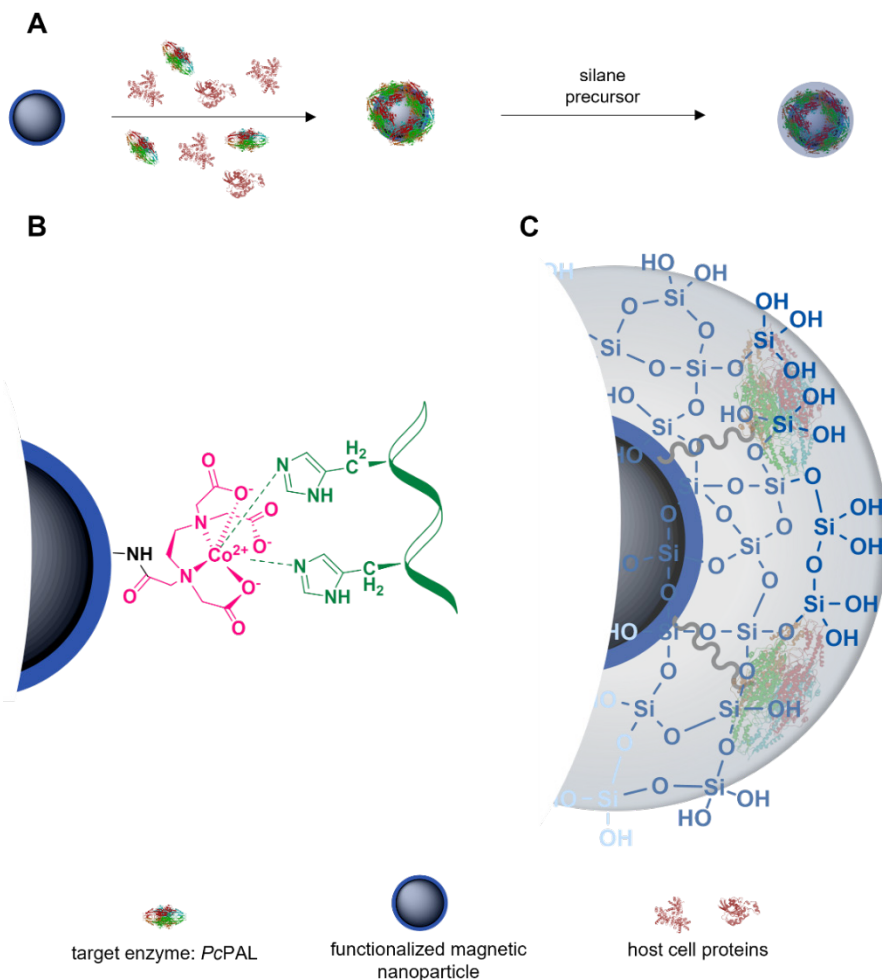


Figure 1. A: Scheme of selective enzyme immobilization and the entrapment of the biocatalyst in sol-gel matrix. **B:** Structure of the surface metal complex binding the histidine tagged protein. **C:** Silica sol-gel matrix entrapment of the *PcPAL* complexed on the surface of the magnetic nanoparticles.

RESULTS AND DISCUSSION

The model enzyme, *PcPAL* with histidine tag was immobilized from the cell lysate on high-capacity magnetic nanoparticles surface-modified with EDTA dianhydride and subsequently complexed with cobalt ions. The magnetic nanoparticles were used at maximum enzyme loading. The immobilization process was monitored in all cases by UV–Vis spectrophotometry, and the enzymatic activity of the supernatant was analyzed before and after the enzyme complexation.

The macroscopic entrapment was investigated by encapsulating the enzyme-loaded magnetic nanoparticles into calcium-alginate beads. Four different biocatalyst loading were tested: 0.5, 1, 5 10 m/m% (AG1–4). Uniform spherical beads were obtained as shown in Figure 2.

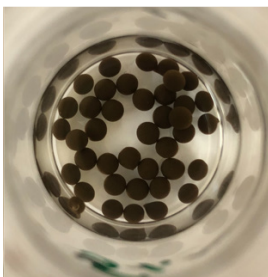


Figure 2. Photograph of the calcium-alginate beads containing entrapped magnetic nanoparticle biocatalysts.

The specific biocatalytic activity of the beads was evaluated in the ammonia elimination reaction (Figure 3.). Since the significant mass contribution of the hydrogel matrix naturally lowers the specific biocatalytic activity [U_B], the conversions of the 30 min reactions were considered for better comparison.

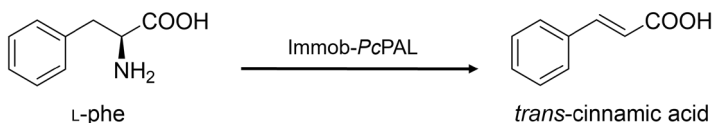


Figure 3. Biocatalytic reaction of immobilized *PcPAL*.

The composite AG3 containing 5 m/m% *PcPAL* complexed nanoparticles proved to be the optimal compromise. Increasing the particle loading to 10% (AG4) no longer improved the activity of the biocatalyst, suggesting that the alginate matrix limited the substrate and product diffusions or the more crowded distribution of the particles limited the enzyme conformational changes needed

to the catalytic activity (Table 1.). To verify the stabilizing effect of the alginate matrix, the beads were washed with 500 mM imidazole, which typically used for protein elution from IMAC resins. The specific biocatalytic activity of the imidazole fractions were tested in the ammonia elimination reaction also and detectable cinnamic acid formation was observed only in case of the non-stabilized biocatalysts confirming that the alginate matrix successfully entrapped the enzyme and prevented its leaching even if the His-tag–metal ion complex was disrupted.

Table 1. Specific biocatalytic activity and enzyme activity of the alginate-entrapped preparations at different loadings (AG1–AG4 represents 0,5; 1; 5; 10 m/m %). All the reactions were performed in triplicates, and the standard deviations were under 5%.

| | U_B [U g ⁻¹] | c [%] |
|------------|-------------------------------|----------|
| MNP | 76.50 | 23.0 |
| AG1 | 0.09 | 2.2 |
| AG2 | 0.15 | 3.6 |
| AG3 | 0.46 | 10.3 |
| AG4 | 0.48 | 13.1 |

Consequently, both entrapment strategies successfully stabilized the PcPAL on the magnetic nanoparticle carrier. The core–shell silica method offering higher specific activity, while the alginate beads provided a macroscopically easier-to-handle formulation.

The sol–gel network formation was then carried out in an aqueous–alcoholic system, using tetraethyl orthosilicate (TEOS) as silane precursor. The effect of the amount of TEOS on catalytic activity was investigated first (27, 54, 107, and 215 μmol TEOS for 1 g magnetic nanoparticle; labeled as SG1-4). The matrix formation occurred overnight at room temperature. During the washing steps following network formation, it became apparent that increasing the TEOS content resulted in progressively more difficult magnetic separation of the catalyst. In addition, silica nanoparticles were formed that no longer contained embedded magnetic particles bearing the immobilized enzyme.

The biocatalytic activity of the stabilized biocatalyst was tested in the same ammonia elimination reaction as previously. The biocatalyst was measured as a suspension into the test reactions, and the exact catalyst

mass was determined retrospectively. The catalytic activity of the silica-coated nanoparticles showed a strong dependence on the precursor concentration, as illustrated in Figure 4.

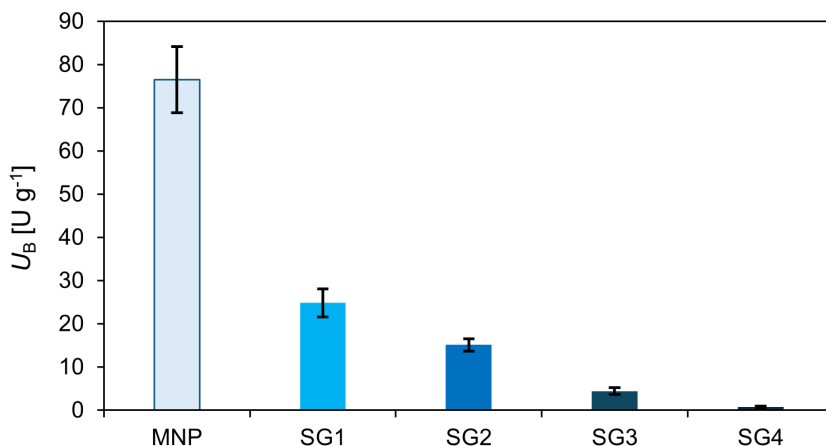


Figure 4. Effect of the silane precursor (TEOS) amount on the specific biocatalytic activity (U_B) of the silica-coated magnetic nanoparticles. (SG1–4 represent increasing TEOS loadings: 27, 54, 107, and 215 μmol TEOS for 1 g magnetic nanoparticle; MNP serves as the non-stabilized control). The measurements were performed in three replicates.

As expected, the formation of a thicker silica shell at higher TEOS loadings (SG3 and SG4) resulted in a dramatic decrease in specific biocatalytic activity, likely due to severe mass transfer limitations that hindered substrate diffusion to the active sites. The sample prepared with the lowest amount of silane (SG1) retained the highest activity; however, even this was significantly lower than that of the non-stabilized reference (MNP). Furthermore, drying the preparations under vacuum caused a substantial loss of activity, indicating the sensitivity of the enzyme to dehydration; therefore, all subsequent samples were stored in buffer suspension.

To improve the catalytic efficiency and alleviate diffusion barriers, the sol–gel matrix was modified by partially substituting TEOS with dimethyldiethoxysilane (DMDEOS). Since DMDEOS contains only two hydrolysable ethoxy groups (Figure 5.), it acts as silica network modifier, creating a less dense matrix.

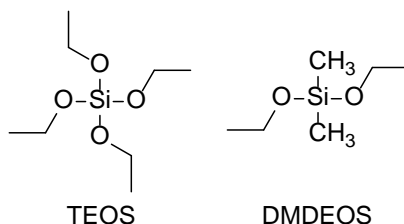


Figure 5. Chemical structures of the silane precursors used for the sol-gel coating: tetraethyl orthosilicate (TEOS) and dimethyldiethoxysilane (DMDEOS).

Optimization studies using the magnetic nanoparticles were performed by varying the TEOS concentration for the SG1 and SG2 precursor quantities. The quantitative results of this optimization are visualized in Figure 6.

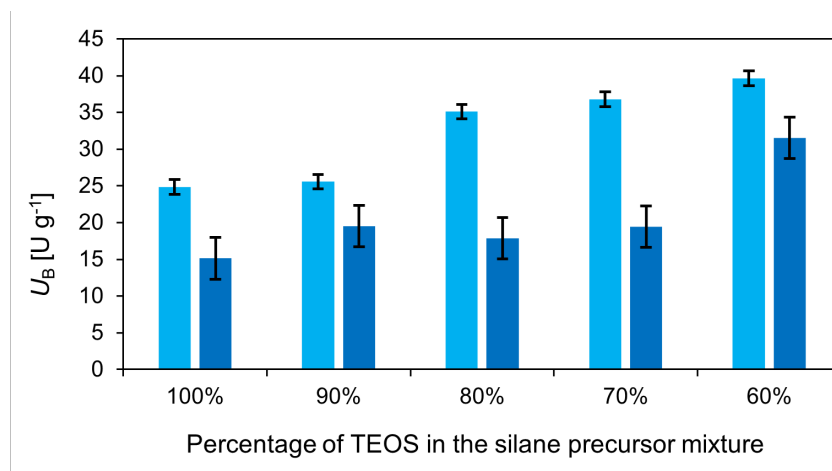


Figure 6. Influence of the TEOS concentration in the silane precursor mixture on the specific biocatalytic activity (■ 27; ■ 54 μmol silane precursor for 1 g magnetic nanoparticle). The measurements were performed in three replicates.

Our results revealed that increasing the DMDEOS ratio up to 40% the specific biocatalytic activity is enhanced. No significant difference was observed between the SG1 samples containing 80, 70 and 60% TEOS. Therefore, the further decrease of TEOS was not investigated. The optimized formulation (60% TEOS – 40% DMDEOS) achieved a specific biocatalytic activity of 39.6 $U\ g^{-1}$. Like the samples stabilized with alginate, the sol-gel matrix provided protection against leaching too; the enzymatic activity in the imidazole washing fractions of sol-gel stabilized MNP biocatalysts were not detectable compared to the free particles.

To assess the operational stability and industrial viability of biocatalysts, reusability studies were conducted using optimized preparations: the silica-coated composite (SG1-60 formulation) and the optimized alginate beads (5 m/m%, AG3). The non-stabilized, enzyme complexed MNP served as the control.

The biocatalysts were subjected to seven consecutive reaction cycles. Between cycles, the biocatalysts were magnetically separated and washed three times with buffer without drying. The operational stability results are presented in Figure 7.

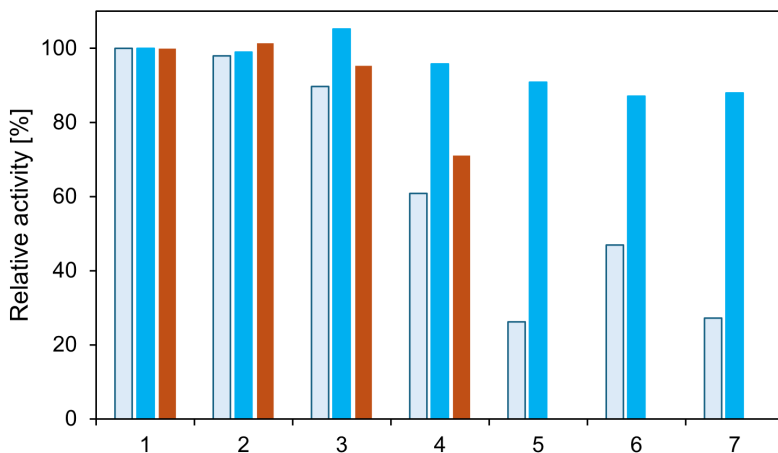


Figure 7. Reusability of the optimized stabilized biocatalysts (■ SG1-60; ■ AG3) compared to the non-stabilized reference (□ MNP) over seven consecutive reaction cycles.

A clear difference in mechanical and operational stability was observed between the carriers. The non-stabilized reference became increasingly difficult to handle after the first few cycles; significant catalyst mass loss was observed during the washing steps, which, combined with enzyme leaching, resulted in a rapid activity decrease, dropping to below 30% by the seventh cycle.

The alginate-entrapped biocatalyst initially performed well but suffered from physical-mechanical instability. As shown in Figure 5, the data series for the alginate beads ends after the fourth cycle. This is because the hydrogel beads began to disintegrate under the mechanical stress of the reaction stirring, making magnetic separation impossible and leading to the termination of the series.

In contrast, the silica-coated biocatalyst (SG1-60) showed high stability and resistance. The particles remained easily separable and chemically stable throughout the experiment. Most notably, the silica-stabilized catalyst retained

more than 80% of its initial activity even after the seventh cycle. This confirms that the porous silica shell not only prevents enzyme leaching, as proved by the imidazole wash tests, but also protects the enzyme from mechanical shear forces.

CONCLUSIONS

In this study, we successfully developed robust magnetic biocatalysts containing recombinant *Petroselinum crispum* phenylalanine ammonia-lyase (PcPAL) to overcome the stability limitations of traditional metal affinity immobilization. We investigated and compared two post-immobilization entrapment strategies: microscopic encapsulation via a sol-gel silica shell and macroscopic entrapment in calcium-alginate hydrogel beads.

Our results demonstrated that the diffusion properties of the silica shell could be significantly improved by the addition of DMDEOS to the silane precursor mixture. The optimized shell formulation (60% TEOS – 40% DMDEOS) successfully balanced the transfer efficiency of small molecules with the enzyme protection, achieving a specific biocatalytic activity of 39.6 U g⁻¹. In case of the alginate entrapment the optimal 5 m/m% biocatalyst loading offered a facile method for creating larger, easy to use biocatalyst beads, but due to the high mass of alginate matrix a lower biocatalytic activity was earned.

The most significant difference between the two stabilized biocatalysts was observed in their operational stability. The alginate beads proved physically unstable under reaction conditions, disintegrating after four reuse cycles. However, the silica-coated nanobiocatalyst exhibited superior mechanical robustness and chemical stability. It completely prevented enzyme leaching and retained more than 80% of its initial catalytic activity even after seven consecutive reaction cycles. Therefore, the formation of a silica shell around the IMAC-immobilized enzyme represents a more effective strategy for the design of industrially viable, reusable magnetic biocatalysts compared to macroscopic hydrogel entrapment.

EXPERIMENTAL SECTION

Materials

Solvents and reagents were purchased from Sigma-Aldrich, Fluka, Merck, Alfa Aesar, Reanal, and Molar Chemicals. Chemicals used for protein analysis were products of Bio-Rad and Thermo Scientific.

The fermentation of the recombinant *PcPAL* enzyme

Production of *PcPAL* was achieved in *E. coli* Rosetta containing the recombinant pET19b plasmid with the gene of *PcPAL* and 10 Histidine. LB-CarCA medium (5 mL; LB medium containing carbenicillin [50 mg L⁻¹], and chloramphenicol [30 mg L⁻¹]) was inoculated with one fresh colony from an overnight LB-CarCA agar plate and cells were grown overnight in shake flask (37 °C, at 200 rpm). Autoinduction medium (0.5 L: Na₂HPO₄, 6 g L⁻¹; KH₂PO₄, 3 g L⁻¹; tryptone, 20 g L⁻¹; yeast extract, 5 g L⁻¹; NaCl, 5 g L⁻¹; glycerol, 7.56 g L⁻¹; glucose, 0.5 g L⁻¹; lactose, 2 g L⁻¹) in a 2 L flask was inoculated with seed culture (2 mL) and was shaken for 16 h at 25 °C, 200 rpm. The cells were harvested by centrifugation (16,000 × g, 4 °C, 20 min), then suspended with 40 mL protease inhibitor containing lysis buffer (50 mM tris(hydroxymethyl)aminomethane, 150 mM NaCl, 0.5 mM EDTA, 2 mM phenylmethylsulfonyl fluoride, 1 mM tris(2-carboxyethyl)phosphine, 1 mM benzamidine). The cell disruption was done using ultrasound, then the media were centrifugated (20,000 × g, 4 °C, 20 min) resulting in the final cell lysate containing recombinant *PcPAL*. To determine the target enzyme concentration as 1 mg mL⁻¹ in the protein mixture a small sample of the cell lysate was purified with Ni Sepharose 6 Fast Flow (Merck GmbH) according to the description provided by the manufacturer.

Synthesis of Magnetic Nanoparticles (MNPs)

Magnetic nanoparticles were synthesized via a solvothermal method. Iron(III) chloride hexahydrate (3.36 g, 12.4 mmol) was dissolved in ethylene glycol (150 mL) via sonication. Subsequently, polyethylene glycol 4000 (12.0 g) and sodium acetate trihydrate (9.0 g, 66.4 mmol) were added to the solution. The mixture was sonicated until complete dissolution, then transferred to a stainless-steel autoclave and heated at 200 °C for 24 h. The resulting black suspension was magnetically separated using a neodymium magnet and the precipitate was washed thoroughly 3 times with distilled water (100 mL) and 3 times with 2-propanol (50 mL). The particles were dried in a fume hood until constant weight.

Preparation of Amine-Functionalized Nanoparticles

The dried magnetic nanoparticles (1500 mg) were dispersed in ethanol (15 mL) containing polyethylene glycol 400 (750 mg) by ultrasonication for 10 min. Ammonium hydroxide solution (35%, 135 µL) was added, and the suspension was shaken for 10 min. Subsequently, 3-(2-aminoethylamino)propyl-methyldimethoxysilane (320 µL, 1.5 mmol) was

added, and the reaction mixture was shaken at room temperature for 24 h. The functionalized particles were washed three times with 2-propanol (10 mL), magnetically separated, and dried in a vacuum chamber at room temperature for 2 hours.

Preparation of the Chelate-type Support

The amine-functionalized particles (200 mg) were dispersed in dimethylformamide (DMF, 7 mL) containing polyethylene glycol 400 (100 mg) via ultrasonication. EDTA-dianhydride (45.6 mg, 178 μmol) and *N*-ethyl-*N,N*-diisopropylamine (30 μL) were added to the suspension. The mixture was shaken at 60 °C for 24 h (600 rpm). Then, distilled water (200 μL) was added, and shaking continued for another 1 h at 60 °C. The particles were washed with acetonitrile (2 \times 5 mL), 2-propanol (1 \times 5 mL), and distilled water (1 \times 5 mL). Finally, the particles were suspended in cobalt(II) chloride solution (5 mL, 50 mM) and were shaken for 30 min at room temperature, washed with distilled water (3 \times 5 mL), 2-propanol (1 \times 5 mL), and dried in a vacuum chamber at room temperature for 2 hours.

Enzyme Immobilization via IMAC

The cobalt-charged magnetic support (50 mg) was suspended in lysis buffer (5 mL; 50 mM Tris, 150 mM NaCl, pH 7.5) and mixed with the cell lysate (5 mL) containing the His-tagged *PcPAL* enzyme. The suspension was shaken for 30 min at room temperature. The immobilization progress was monitored by measuring the activity of the supernatant; fresh lysate was added until saturation was reached. The immobilized biocatalyst was magnetically separated and washed sequentially with LS buffer (50 mM HEPES, 30 mM KCl, pH 7.5), HS buffer (50 mM HEPES, 300 mM KCl, pH 7.5), and Tris buffer (50 mM, pH 7.5).

Sol-Gel Silica Coating of the Biocatalyst

The immobilized biocatalyst suspension (1600 μL containing 10 mg particles) was mixed with polyethylene glycol 1000 solution (400 μL , 5 m/m% in 50 mM Tris buffer, pH 7.5). To this mixture, 2-propanol (250 μL) and the appropriate amount of silane precursors (see at Table 2 and 3.) were added. Polycondensation was initiated by adding NaF catalyst (20 μL , 1 M). After shaking for 24 h at room temperature, the silica-coated particles were magnetically separated and washed twice with 25% 2-propanol in Tris buffer, then stored in Tris buffer (50 mM, pH 7.5).

Table 2. Amount of TEOS during the silica shell optimization.

| | SG1 | SG2 | SG3 | SG4 |
|-------------------------------|------------|------------|------------|------------|
| TEOS [μL] | 60 | 120 | 240 | 480 |

Table 3. Amounts of TEOS and DMDEOS during the second silica shell optimization.

| | | | TEOS ratio [%] | | | |
|------------|---------------|-------------------|-----------------------|-----------|-----------|-----------|
| | | | 90 | 80 | 70 | 60 |
| SG1 | TEOS | [μL] | 54 | 48 | 42 | 36 |
| | DMDEOS | [μL] | 4.6 | 9.2 | 13.8 | 18.4 |
| SG2 | TEOS | [μL] | 108 | 96 | 84 | 72 |
| | DMDEOS | [μL] | 9.2 | 18.4 | 27.6 | 36.9 |

Entrapment in Alginate Beads

The immobilized biocatalyst suspension (corresponding to 0.5–10 m/m% loading) was mixed with sodium alginate solution (1 g, 30 mg mL⁻¹ in water) and 1000 μL Tris buffer (100 mM, pH 7.5). The mixture was homogenized by vortex and added dropwise into a 2% CaCl₂ solution using a syringe with a blunt-end needle. The resulting magnetic beads were separated, washed three times with Tris buffer (10 mL, 50 mM, pH 7.5), and stored at 4 °C.

Activity Measurements

The biocatalytic activity was determined in the ammonia elimination reaction of L-phenylalanine. The biocatalyst (2.5–5 mg) was added to L-phenylalanine solution (1 mL, 10 mM in 100 mM Tris buffer, pH 8.8) and shaken at 30 °C (600 rpm). Samples (20 μL) were taken after 30, 60 and 120 minutes, diluted with distilled water (280 μL), and the absorbance of the produced *trans*-cinnamic acid was measured at 290 nm using a microplate reader [Thermo Scientific Multiscan SkyHigh microplate reader, (Thermo Fisher Scientific Inc., Waltham, MA, USA)].

Characterization of the productivity and immobilization yield

To characterize the productivity of the different biocatalysts, the specific biocatalytic activity was calculated using the equation

$$U_B = n_P / (t \times m_B) \quad (1)$$

where n_P [μmol] is the amount of the product, t [min] is the reaction time and m_B [g] is the mass of the applied biocatalyst. To determine the ratio of immobilized target enzyme the activity of the crude cell lysate was measured before and after the immobilization process as well as the imidazole elution fractions during the washing steps.

ACKNOWLEDGMENTS

Balint Alacs acknowledges the support of Gedeon Richter Talentum Foundation.

REFERENCES

1. J. M. Guisan; F. López-Gallego; L. Betancor; C. Mateo; V. Grazu; G. Fernandez-Lorente; J. Rocha-Martin; J. M. Bolivar; K. Ovsejevi; C. Manta; et al. *Immobilization of Enzymes and Cells*; Guisan, J.M., Ed.; Methods in Molecular Biology; Humana Press: Totowa, NJ, **2013**; Vol. 1051; ISBN 978-1-62703-549-1.
2. Sheldon, R.A. Fundamentals of Green Chemistry: Efficiency in Reaction Design. *Chem. Soc. Rev.* **2012**, *41*, 1437–1451, doi:10.1039/C1CS15219J.
3. Bornscheuer, U.T.; Huisman, G.W.; Kazlauskas, R.J.; Lutz, S.; Moore, J.C.; Robins, K. Engineering the Third Wave of Biocatalysis. *Nature*, **2012**, *485*, 185–194, doi:10.1038/nature11117.
4. Cui, J.D.; Qiu, J.Q.; Fan, X.W.; Jia, S.R.; Tan, Z.L. Biotechnological Production and Applications of Microbial Phenylalanine Ammonia Lyase: A Recent Review. *Crit. Rev. Biotechnol.* **2014**, *34*, 258–268, doi:10.3109/07388551.2013.791660.
5. Datta, S.; Christena, L.R.; Rajaram, Y.R.S. Enzyme Immobilization: An Overview on Techniques and Support Materials. *3 Biotech*, **2013**, *3*, 1–9, doi:10.1007/s13205-012-0071-7.
6. Mateo, C.; Palomo, J.M.; Fernandez-Lorente, G.; Guisan, J.M.; Fernandez-Lafuente, R. Improvement of Enzyme Activity, Stability and Selectivity via Immobilization Techniques. *Enzyme Microb. Technol.*, **2007**, *40*, 1451–1463, doi:10.1016/j.enzmictec.2007.01.018.
7. Gupta, A.K.; Gupta, M. Synthesis and Surface Engineering of Iron Oxide Nanoparticles for Biomedical Applications. *Biomaterials*, **2005**, *26*, 3995–4021, doi:10.1016/j.biomaterials.2004.10.012.
8. Lu, A.-H.; Salabas, E.L.; Schüth, F. Magnetic Nanoparticles: Synthesis, Protection, Functionalization, and Application. *Angewandte Chemie International Edition*, **2007**, *46*, 1222–1244, doi:10.1002/anie.200602866.

9. Lucena, G.N.; Santos, C.C. dos; Pinto, G.C.; Piazza, R.D.; Guedes, W.N.; Jafelicci Júnior, M.; de Paula, A. V.; Marques, R.F.C. Synthesis and Characterization of Magnetic Cross-Linked Enzyme Aggregate and Its Evaluation of the Alternating Magnetic Field (AMF) Effects in the Catalytic Activity. *J. Magn. Magn. Mater.*, **2020**, *516*, 167326, doi:10.1016/j.jmmm.2020.167326.
10. Porath, J.; Carlsson, J.; Olsson, I.; Belfrage, G. Metal Chelate Affinity Chromatography, a New Approach to Protein Fractionation. *Nature*, **1975**, *258*, 598–599, doi:10.1038/258598a0.
11. Sánta-Bell; Molnár; Varga; Nagy; Hornyánszky; Paizs; Balogh-Weiser; Poppe “Fishing and Hunting”—Selective Immobilization of a Recombinant Phenylalanine Ammonia-Lyase from Fermentation Media. *Molecules*, **2019**, *24*, 4146, doi:10.3390/molecules24224146.
12. Cassimjee, K.E.; Kourist, R.; Lindberg, D.; Wittrup Larsen, M.; Thanh, N.H.; Widersten, M.; Bornscheuer, U.T.; Berglund, P. One-step Enzyme Extraction and Immobilization for Biocatalysis Applications. *Biotechnol. J.*, **2011**, *6*, 463–469, doi:10.1002/biot.201000357.
13. Weiser, D.; Nagy, F.; Bánóczy, G.; Oláh, M.; Farkas, A.; Szilágyi, A.; László, K.; Gellért, Á.; Marosi, G.; Kemény, S.; et al. Immobilization Engineering – How to Design Advanced Sol–Gel Systems for Biocatalysis? *Green Chemistry*, **2017**, *19*, 3927–3937, doi:10.1039/C7GC00896A.
14. Appert, C.; Logemann, E.; Hahlbrock, K.; Schmid, J.; Amrhein, N. Structural and Catalytic Properties of the Four Phenylalanine Ammonia-Lyase Isoenzymes from Parsley (*Petroselinum Crispum* Nym.). *Eur. J. Biochem.*, **1994**, *225*, 491–499, doi:10.1111/j.1432-1033.1994.00491.x.
15. Poppe, L.; Rétey, J. Friedel–Crafts-Type Mechanism for the Enzymatic Elimination of Ammonia from Histidine and Phenylalanine. *Angewandte Chemie International Edition*, **2005**, *44*, 3668–3688, doi:10.1002/anie.200461377.